Developmental and Comparative Immunology 148 (2023) 104917

Contents lists available at ScienceDirect

Developmental and Comparative Immunology

journal homepage: www.elsevier.com/locate/devcompimm

The phenylalanine-28 is crucial for black carp RIG-I mediated antiviral signaling

Ji Liu [a,b], Yixuan He [a], Yujia Miao [a], Chushan Dai [a], Jun Yan [a,b], Meiling Liu [b], Jun Zou [c], Hao Feng [a,*]

[a] State Key Laboratory of Developmental Biology of Freshwater Fish, College of Life Science, Hunan Normal University, Changsha, 410081, China
[b] College of Chemistry and Chemical Engineering, Hunan Normal University, Changsha, 410081, China
[c] Key Laboratory of Exploration and Utilization of Aquatic Genetic Resources, Ministry of Education, Shanghai Ocean University, Shanghai, 201306, China

ARTICLE INFO

Keywords:
Innate immunity
RIG-I
Interferon
Black carp

ABSTRACT

Retinoic acid-inducible gene I (RIG-I) functions as a cytosolic sensor to recognize RNA products of the invading microorganisms and induce the production of type I interferons (IFNs) . In this study, two RIG-I variants, named as bcRIG-Ia and bcRIG-Ib, were characterized in black carp (*Mylopharyngodon piceus*) respectively. RNA pull-down assay revealed that both bcRIG-Ia and bcRIG-Ib could bind to synthetic poly(I:C) and the RD domain was crucial for RNA binding of these two molecules. However, over-expression of bcRIG-Ib, but not bcRIG-Ia, induced the transcription of IFN promoter, and led to the improved antiviral activity against both spring viremia of carp virus (SVCV) and grass carp reovirus (GCRV). And knockdown of bcRIG-I dampened the transcription of bcViperin and bcIFNb in host cells. Truncation mutation and site mutation analysis identified that phenylalanine (F)- 28 was crucial for bcRIG-Ib oligomerization and its mediated IFN signaling. Interestingly, F28 was conserved among teleost RIG-Is and site mutation analysis revealed that F28 was essential for RIG-I mediated IFN signaling in the cyprinid fish. Thus, our study concludes that F28 is crucial for black carp RIG-I mediated antiviral signaling and suggests F28 is also essential for the activation of IFN signaling by RIG-Is from other teleost fish.

1. Introduction

The innate immune system, as the first barrier, plays a key role in the defense against pathogenic microorganisms through a limited number of germline-encoded pattern recognition receptors (PRRs) (Meylan et al., 2006; Takeuchi and Akira, 2010). The PRRs recognize pathogens associated molecular patterns (PAMPs), including nucleotides, proteins and lipids, and induce the production of interferons (IFNs), inflammatory factors, and pro-inflammatory factors through signaling cascade, which ultimately initiate the innate immune response Liu and Cao (2016); Elward and Gasque (2003). The PRRs contain Toll-like receptors (TLRs), NOD-like receptors (NLRs), RIG-I-like receptors (RLRs) and so on (Broz and Monack, 2013). TLRs locate on the cell surface or lysosome/endosome membranes, recognizing lipids and nucleic acid. In contrast, RLRs mainly sense viral molecules in the cytoplasm (Akira et al., 2006).

RIG-I (also known as DDX58) is a member of RLR family and composes of three main domains: two N-terminal CARD domains, the central DExDc/H domain and the C-terminal RD domain (Yoneyama et al., 2005; Kolakofsky et al., 2012; Leung and Amarasinghe, 2012). In resting cells, RIG-I is kept in an autoinhibition state via intramolecular interaction between the CARD domains and the helicase domain (Kolakofsky et al., 2012; Saito et al., 2007). Upon viral infection, RNA-binding perturbs this auto-inhibiting interaction, releasing the N-terminal CARD domains (Kowalinski et al., 2011; Luo et al., 2011). The exposed CARD domain of RIG-I interacts with mitochondrial antiviral signaling protein (MAVS), activating the downstream signaling and IFNs production (Peisley et al., 2013; Stetson and Medzhitov, 2006). Together, these signaling cascades constitute a powerful innate immune response that establishes an antiviral state in the early stages of infection. Further, RIG-I deficiency in mice severely damages host defense and greatly increases viral replication (Kato et al., 2006).

Over the last decade, teleost homologues of mammalian RIG-I have been identified and their roles in innate immunity have been investigated in teleost fish, including zebrafish (*Danio rerio*) (Zou et al., 2015) , grass carp (*Ctenopharyngodon idella*) (Chen et al., 2012) and so on. Overexpression of zebrafish RIG-Ib, but not RIG-Ia, resulted in the

* Corresponding author.
E-mail address: fenghao@hunnu.edu.cn (H. Feng).

https://doi.org/10.1016/j.dci.2023.104917
Received 5 July 2023; Received in revised form 12 August 2023; Accepted 13 August 2023
Available online 15 August 2023

Table 1
Primers used in the study.

Primer name	Sequence (5′-3′)	Primer information
bcRIG-Ia-F	ACTGACGGTACCGCCACCATGTACGAGATGCAAAAGGAGAATT	ORF cloning
bcRIG-Ib-F	ACTGACGGTACCGCCACCATGTACGAGCTGGAAAAGGAGAATT	
bcRIG-Ia/b-R	ACTGACCTCGAGGTCTCTCAGCGGCCATGT	
a(MQL-LEF)-F	ACTGACGGTACCGCCACCATGTACGAGATGCAAAAGGAGAATTTGCGGCGCTTGAGCGATTATATCGCGCAGTTTTTACAACCGTCACTTATCAAAACCCTCATGACG	Mutant construction
b(LEF-MQL)-F	ACTGACGGTACCGCCACCATGTACGAGCTGGAAAAGGAGAATTTGCGGCGCTTGAGCGATTATATCGCGCAGTTTTTACAACCGTCACTTATCAAAACCTTCATGACG	
a(M4L)-F	ACTGACGGTACCGCCACCATGTACGAGCTGCAAAAGGAG	
a(Q5E)-F	ACTGACGGTACCGCCACCATGTACGAGATGGAAAAGGAG	
a(L28F)-F	ACTGACGGTACCGCCACCATGTACGAGATGCAAAAGGAGAATTTGCGGCGCTTGAGCGATTATATCGCGCAGTTTTTACAACCGTCACTTATCAAAACCTTCATGACG	
a/b-CARD-R	ACTGACCTCGAGTCATCCATTGGACTCCAGCAGCTCCAGC	
b(F28L)-F	ACTGACGGTACCGCCACCCTTATCAAAACCCTGATGACGACG	
b(F28L)-R	ACTGACCTCGAGATCAAAGTACGTCGTCATCAGGGTTTTGAT	
bcRIG-I-△RD-R	ACTGACCTCGAGGCGTGTTTTGGGTTTGTCGGGAC	
eRIG-I-F	ACTGACGGTACCGCCACCATGTACGAGATGGAAAAGG	
eRIG-I-R	ACTGACCTGCAGTCAGTCTCTCAGCGGCCATG	
eRIG-I(F28L)-F1	ATCAAAACCTTAATGACGACG	
eRIG-I(F28L)-R1	CGTCGTCATTAAGGTTTTGAT	
eRIG-I-2CARD-R1	ACTGACGCGGCCGCtcaTCCATTGGACTCCAGCAGCTC	
DrRIG-I- (F28L) -F	ACTGACACTAATAAAAACCCTTATGACGACATAC	
DrRIG-I- (F28L) -R	ACTGACGTATGTCGTCATAAGGGTTTTTATTAGT	
DrRIG-I-2CARD-R1	ACTGACGCGGCCGCtcaTGACTTTCTTGTCTCCAG	
CMV	CGCAAATGGGCGGTAGGCGTG	
BGH	TAGAAGGCACAGTCGAGG	
shRNA		
shbcRIG-I-1-F	CCGGGGGAATATCAGAAGGAGTTGACTCGAGTCAACTCCTTCTGATATTCCCTTTTT G	shRNA-bcRIG-I-1
shbcRIG-I-1-R	AATTCAAAAAGGGAATATCAGAAGGAGTTGACTCGAGTCAACTCCTTCTGATATTCCC	
shbcRIG-I-2-F	CCGGGGTCGACGTCTATGAACAACACTCGAGTGTTGTTCATAGACGTCGACC TTTTT G	shRNA-bcRIG-I-2
shbcRIG-I-2-R	AATTCAAAAAGGTCGACGTCTATGAACAACACTCGAGTGTTGTTCATAGACGTCGACC	
shbcRIG-I-3-F	CCGGGCAGAGAACTCTACAACTACACTCGAGTGTAGTTGTAGAGTTCTCTGC TTTTT G	shRNA-bcRIG-I-3
shbcRIG-I-3-R	AATTCAAAAAGCAGAGAACTCTACAACTACACTCGAGTGTAGTTGTAGAGTTCTCTGC	
U6	ACTATCATATGCTTACCGT	
PLKO.1-R	CTATTCTTTCCCCTGCACTG	
q-PCR		
bcactin-Q-F	TGGGCACCGCTGCTTCCT	ex vivo q-PCR
bcactin-Q-R	TGTCCGTCAGGCAGCTCAT	
bcMx1-Q-F	TGAGCGTAGGCATTAGCAC	
bcMx1-Q-R	CCTGGAGCAGCAGATAGCG	
bcViperin-Q-F	CCAAAGAGCAGAAAGAGGGACC	
bcViperin-Q-R	TCAATAGGCAAGACGAACGAGG	
bcIFNb-Q-F	GACCACGTTTCCATATCTTT	
bcIFNb-Q-R	CATTTTTTCTTCATCCCACT	
bcRIG-I-Q-F	AATTGCGACACTCACCAGCAG	
bcRIG-I-Q-R	AGCATAATCAGGAACATCATACG	
SVCV-G-Q-F	GATGACTGGGAGTTAGATGGC	
SVCV-G-Q-R	ATGAGGGATAATATCGGCTTG	
SVCV-N-Q-F	GGTGCGAGTAGAAGACATCCCCG	
SVCV-N-Q-R	GTAATTCCCATCATTGCCCCAGAC	
SVCV-P-Q-F	AACAGGTATCGACTATGGAAGAGC	
SVCV-P-Q-R	GATTCCTCTTCCCAATTGACTGTC	

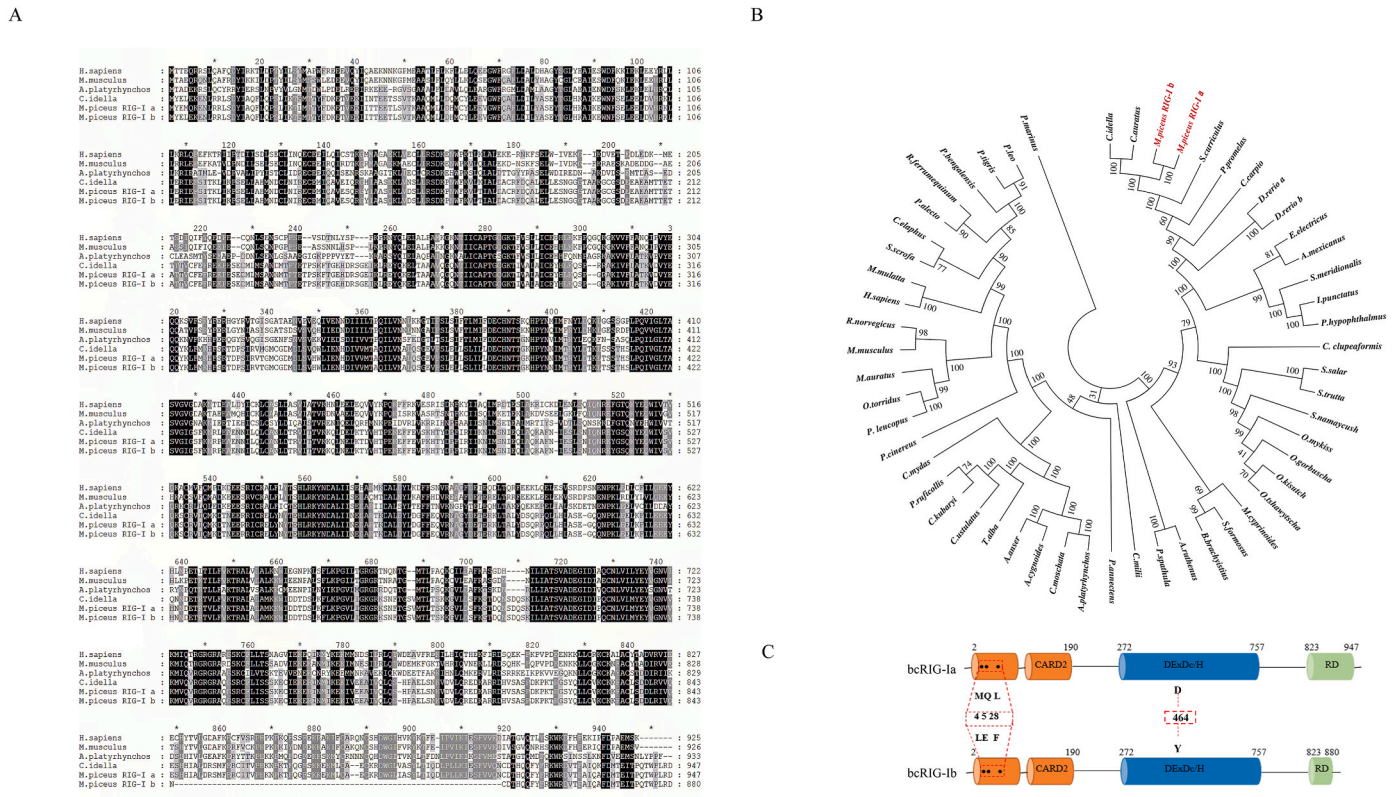

Fig. 1. Sequence analysis of bcRIG-Ia and bcRIG-Ib. (A) Amino acid sequence alignment of bcRIG-I with RIG-I homologues from other vertebrates, which was performed by using bioinformatics software MEGA6.0 and GENEDOC. (B)Phylogenetic tree was generated from vertebrate RIG-I of different species by using MEGA 6.0 program, which were same to those in Table 2 (C) Diagrams the functional domains of bcRIG-Ia and bcRIG-Ib.

significant increase of the transcription of IFN promoter and the induced expression of IRF7 and Mx, thus protecting the cells against SVCV infection (Zou et al., 2015). Simultaneously, knockdown of RIG-I specifically repressed the induction of group II IFNs (IFNφ2, IFNφ3) by nervous necrosis virus(NNV) infection in zebrafish cells (Chen et al., 2015). However, there are few studies about the activation and regulation teleost RIG-I.

In the present study, two RIG-I homologues have been cloned and characterized from black carp, named bcRIG-Ia and bcRIG-Ib respectively. bcRIG-Ib, but not bcRIG-Ia, induced the IFN promoter transcription in reporter assay and presented the antiviral activity in plaque assay. Mutation analysis demonstrated that phenylalanine- 28 was essential for bcRIG-Ib oligomerization, which explained the functional difference between bcRIG-Ia and bcRIG-Ib in IFN signaling. Interestingly, F28 was conserved among teleost RIG-Is, and mutation analysis revealed that F28 was also critical for RIG-I mediated IFN signaling in the cyprinid fish. Thus, our data shed a new light on the RIG-I regulation during antiviral innate immunity in vertebrates.

2. Material and methods

2.1. Cells, plasmids and viruses

Human embryonic kidney 293T (HEK293T), *Epithelioma papulosum cyprinid* (EPC), *Ctenopharyngodon idella* kidney (CIK) and *M. piceus* kidney (MPK) cells were grown in Dulbecco's modified Eagle's medium (DMEM) supplemented with 10% fetal bovine serum (FBS), 2 mM-glutamine, and 100U/ml penicillin and 100 mg/ml streptomycin. HEK293T cells were cultured at 37 °C, while EPC, CIK and MPK cells were cultured at 26 °C, all with 5%CO_2. Polyethylenimine (PEI) was used for HEK293T and EPC transfection, while MPK cells were transfected by using Lipomax (SUDGEN).

pcDNA5/FRT/TO, pcDNA5/FRT/TO-Flag-bcMAVS, pcDNA5/FRT/TO-HA-Ub, pRL-TK, Luci-bcIFNa (for black carp IFNa promoter activity analysis) and luci-DrIFNφ3 (for zebrafish IFNφ3 promoter activity analysis) were kept in the laboratory. The open reading frame (ORF) of bcRIG-Ia or bcRIG-Ib was cloned based on the total RNA from the spleen of black carp and inserted into pcDNA5/FRT/To with a HA tag or a Flag tag at the C-terminus separately. shRNAs targeting both bcRIG-Ia and bcRIG-Ib were inserted into PLKO.1, which were designed according to the protocol on the website (http://rnaidesigner.thermofisher.com/rnaiexpress). All constructed plasmids were verified by sequencing analysis and the primers with the information of restricted enzyme sites were listed in Table 1. Plasmids expressing RIG-I from grass carp (CiRIG-I) and zebrafish (DrRIG-I) were kind gifts from Dr. Jianguo Su (College of Fisheries, Huazhong Agricultural University) and Dr. Mingxian Chang (Institute of Hydrobiology, Chinese Academy of Sciences), separately.

Grass carp reovirus (GCRV, strain: GCRV873) and spring viremia of carp virus (SVCV, strain: SVCV741) were kept in the lab, which were propagated in CIK and EPC cells in the presence of 2% FBS at 26 °C respectively. Virus titer was determined by the plaque assay using EPC cells as previously described (Wu et al., 2019; Wang et al., 2021). Briefly, the virus was applied to 10-fold serial dilution and the array of the diluted virus was added to EPC cells. After 2 h incubation, the media were changed with fresh DMEM containing 2% FBS and 0.75% methylcellulose. And the plaques were measured at the third day post-infection.

2.2. Quantitative real-time PCR

The relative mRNA levels of genes, including *bcIFNb*, *bcViperin*, *bcMx1* *SVCV-G*, *SVCV-N* and *SVCV-P* were examined through

Table 2
Comparison of bcRIG-Ib with other vertebrate RIG-I (%).

Species	GenBank accession number	Full-length sequence	
		Identity	Similarity
Mylopharyngodon piceus b	OQ407684	100.0	100.0
Mylopharyngodon piceus a	OQ407685	99.5	99.8
Ctenopharyngodon idella	JX649222.1	97.8	98.6
Carassius auratus	JF970225.1	97.3	98.1
Squaliobarbus curriculus	MK759919.1	94.3	96.9
Pimephales promelas	XM_039679108.1	83.7	91.3
Cyprinus carpio	HQ850439.1	81.6	89.4
Danio rerio a	JX462558.1	76.2	86.2
Danio rerio b	JX462559.1	72.4	81.9
Electrophorus electricus	XM_027030455.2	66.8	80.4
Astyanax mexicanus	XM_022662151.2	67.2	80.0
Pangasianodon hypophthalmus	XM_053240887.1	62.9	76.0
Megalops cyprinoides	XM_036551271.1	63.2	77.5
Ictalurus punctatus	OP805912.1	63.2	78.0
Salvelinus namaycush	XM_038983940.1	59.8	74.9
Silurus meridionalis	XM_046870130.1	63.4	77.4
Salmo trutta	XM_029754686.1	60.3	75.3
Oncorhynchus tshawytscha	XM_042327984.1	60.2	74.8
Oncorhynchus mykiss	XM_036973405.1	59.8	74.7
Oncorhynchus kisutch	XM_031791579.1	59.6	74.2
Oncorhynchus gorbuscha	XM_046870130.1	59.6	74.7
Salmo salar	NP_001157171.1	60.6	75.7
Coregonus clupeaformis	XM_045211895.1	58.8	73.4
Scleropages formosus	XM_018738536.2	57.0	73.5
Brienomyrus brachyistius	XM_048970065.1	55.3	72.6
Polyodon spathula	XM_041221503.1	55.5	72.7
Acipenser ruthenus	XM_034015560.2	55.1	72.9
Cervus elaphus	XM_043890595.1	47.0	65.9
Callorhinchus milii	XM_007906608.2	46.3	65.3
Protopterus annectens	XM_044061005.1	49.0	65.1
Rhinolophus ferrumequinum	XM_033123991.1	46.8	66.1
Panthera leo	XM_042913443.1	46.4	65.2
Panthera tigris	XM_007076591.3	46.4	65.2
Prionailurus bengalensis	XM_043565840.1	46.3	65.2
Pteropus alecto	NP_001277087.1	46.6	66.4
Homo sapiens	NP_055129.2	46.4	66.9
Macaca mulatta	NP_001036133.1	46.7	66.5
Mesocricetus auratus	NP_001297482.1	45.7	65.3
Onychomys torridus	XM_036177519.1	45.5	65.7
Mus musculus	NP_766277.3	45.3	65.6
Rattus norvegicus	NM_001395071.1	45.6	65.5
Peromyscus leucopus	XM_028884064.2	45.0	65.9
Phascolarctos cinereus	XM_020976230.1	45.7	65.8
Chelonia mydas	XM_043547762.1	46.8	64.4
Sus scrofa	NP_998969.2	45.8	65.3
Catharus ustulatus	XM_033084725.2	44.1	62.6
Corvus kubaryi	XM_042023561.1	44.7	62.9
Cairina moschata	KF669395.1	43.9	63.4
Anas platyrhynchos	NP_001297309.1	44.1	63.6
Pyrgilauda ruficollis	XM_041486418.1	44.7	63.2
Anser cygnoides	NP_001298119.1	44.4	63.4
Tyto alba	XM_033000985.2	44.8	63.1
Anser anser	JF804977.1	43.7	62.7
Petromyzon marinus	XM_032971795.1	35.4	55.9

quantitative real-time PCR (qRT-PCR) by using Applied Biosystems QuantStudio 5 Real-Time PCR Systems (Thermo Fisher, USA). The primes for qRT-PCR were listed in Table 1 and qRT-PCR program was: 1 cycle of 95 °C/10 min, 40 cycles of 95 °C/15 s, 60 °C/1 min. The data was analyzed by the 2-ΔΔCT method as previously described (Wang et al., 2021).

2.3. Immunoblotting and Co-immunoprecipitation

The transfected HEK293T cells or EPC cells were harvested at 48 h post-transfection and lysed for immunoblotting (IB) as previously described (Zhou et al., 2015). Briefly, the whole cell lysates were isolated by 8% SDS-PAGE and transferred to PVDF membrane. The transferred membranes loading the target proteins were probed with mouse anti-Flag or mouse anti-HA monoclonal antibody (Sigma), and followed by incubation with the secondary antibody. Finally, NBT/BCIP alkaline phosphatase substrate (Thermo Fisher) was used for visual analysis of target proteins.

The transfected HEK293T cells in 10 cm plate were collected at 48 h post-transfection and lysed for co-immunoprecipitation (Co-IP) assay as previously described (Wu et al., 2019). Briefly, the whole cell lysates were incubated with protein A/G agarose beads (Sigma) for 1 h at 4 °C. After precleaning and concentration, the anti-Flag conjugated protein A/G agarose beads (Sigma) were added and incubated with the supernatant media at 4 °C for 4 h. The beads were heated-denatured in 5 × SDS-sample buffer after 4 times wash with 1% NP-40 lysis buffer and used for IB as above.

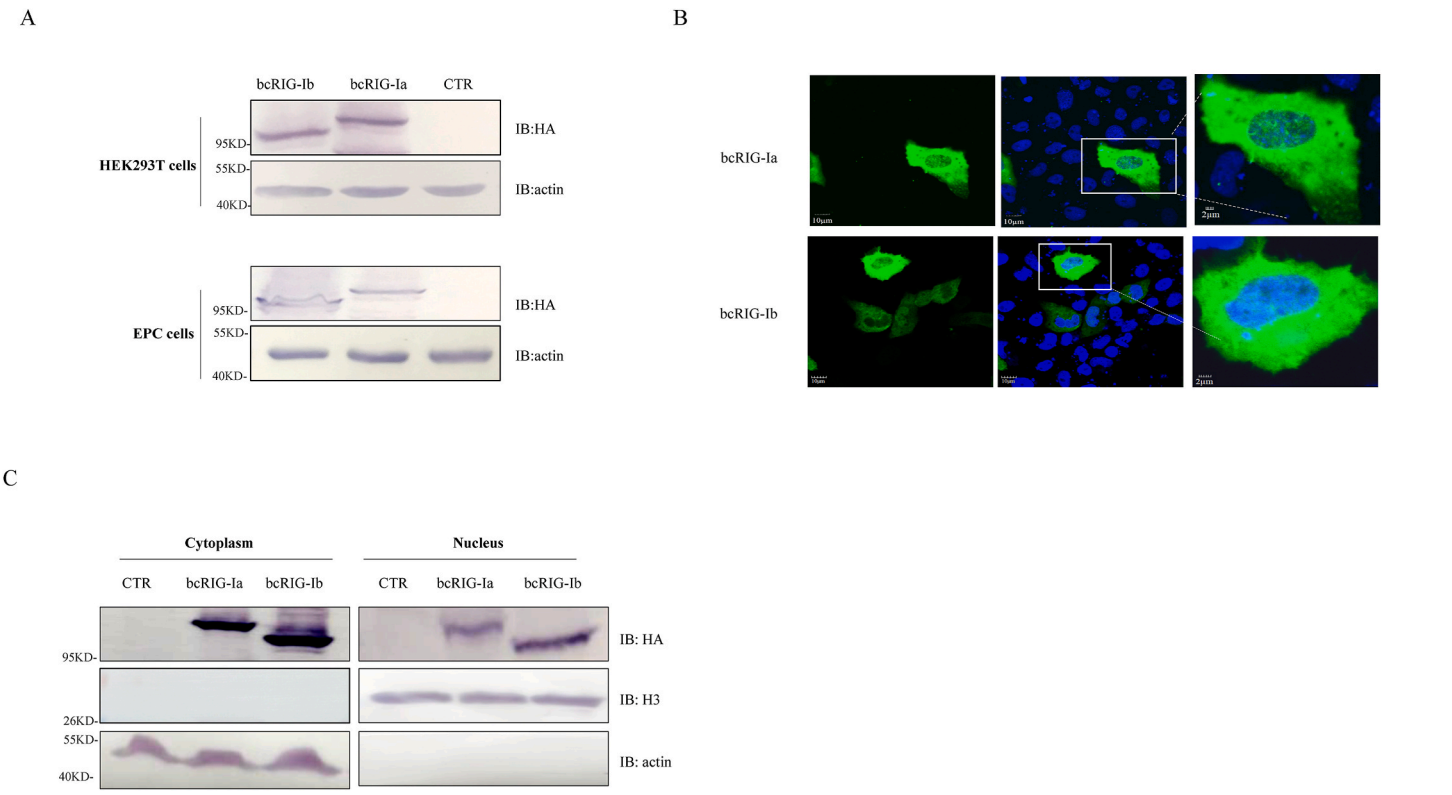

Fig. 2. Protein expression and subcellular distribution of bcRIG-Ia and bcRIG-Ib. (A) HEK293T cells or EPC cells in 6-well plate were transfected with bcRIG-Ia, bcRIG-Ib or the empty vector (3 μg), and applied to IB. (B) EPC cells in 24-well plate were transfected with bcRIG-Ia or bcRIG-Ib (300 ng), then the transfected cells were used for immunofluorescence staining. The bars stand for the scale of 2 μm or 10 μm separately. (C) EPC cells in 6-well plate were transfected with bcRIG-Ia , bcRIG-Ib or the empty vector (3 μg) and applied to the nucleus-cytoplasm extraction. CTR: pcDNA5/FRT/TO; bcRIG-Ia:pcDNA5/FRT/TO-bcRIG-Ia-HA; bcRIG-Ib: pcDNA5/FRT/TO-bcRIG-Ib-HA.

2.4. Immunofluorescence microscopy

The transfected cells were fixed with 4% (v/v) paraformaldehyde at 24 h post-transfection. The fixed cells were permeabilized with 0.2% Triton X-100 and used for immunofluorescent staining as previously described (Yang et al., 2019). Briefly, the anti-HA antibody was probed at the ratio of 1:500; Alexa 488-conjugated secondary antibody was probed at the ratio of 1:1000; DAPI was used for nucleus staining.

2.5. Semi-denaturing detergent agarose gel electrophoresis (SDD-AGE)

The oligomerization of bcRIG-I or bcRIG-I mutants was analyzed by SDD-AGE according to the published protocol (Hou et al., 2011). Briefly, the transfected cells were lysed with 1%NP-40 lysis buffer, and resuspended in 4 × sample buffer for 15 min at room temperature. After centrifugation, the supernatant was mixed with 4 × loading buffer. The samples were loaded into horizontal 1.5% agarose gel made with 1 × TBE with 0.1% SDS. After gel electrophoresis at 100V for approximately 90min at 4 °C, the proteins were transferred to PVDF membrane for immunoblotting as above.

2.6. RNA pull-down assay

The transfected HEK293T cells were lysed for 15min in HNTG buffer (20 mM HEPES PH 7.9, 150 mM NaCl, 1%TritonX-100, 10% glycerin, 1 mM MgCl2 and 2 mM EDTA) with protease inhibitors on ice, cell lysates were clarified by centrifugation at 12000*g* for 5min at 4 °C. Biotin-labeled poly(I:C) (Invivogen) was added to the lysates and incubated with the lysates for overnight at 4 °C. Cell lysates were then mixed with streptavidin agarose beads (sigma) for 2 h at 4 °C. After incubation, the beads were thrice washed with ice-cold HNTG buffer, and eluted by heating at 95 °C for 15 min with 5 × sample buffer and analyzed by IB (Vegna et al., 2016).

2.7. Nuclear and cytoplasmic protein extraction

The transfected EPC cells were harvested at 48 h after transfection and lysed in 0.5% NP-40 lysis buffer with protease inhibitor for 10 min on ice. The lysates were clarified by centrifugation at 700*g* for 5 min, the precipitate (nucleus) was eluted by heating at 95 °C for 15 min with 5 × sample buffer, the supernatant then was transferred to a new tube and centrifuged at 12000g for 2 min. After centrifugation, the supernatant (cytoplasm) also was heated-denatured in 5 × sample buffer and used for IB as above.

2.8. Statistical analysis

For the statistics analysis of the data of qRT-PCR, reporter assay and viral titration, all data were obtained from three independent experiments with each performed in triplicate. Error bars represent the standard error of the mean (+SEM) of three independent experiments. The two-tailed student's t-test was used for a comparison of three independent experiments. A p-value <0.05 was considered statistically significant (*); a p-value<0.01 was considered statistically highly significant (**).

3. Results

3.1. Cloning and sequence analysis of bcRIG-Ia and bcRIG-Ib

To explore the role of RIG-I in the antiviral innate immunity of black carp, the open reading frames (ORFs) of two RIG-I transcripts, named as

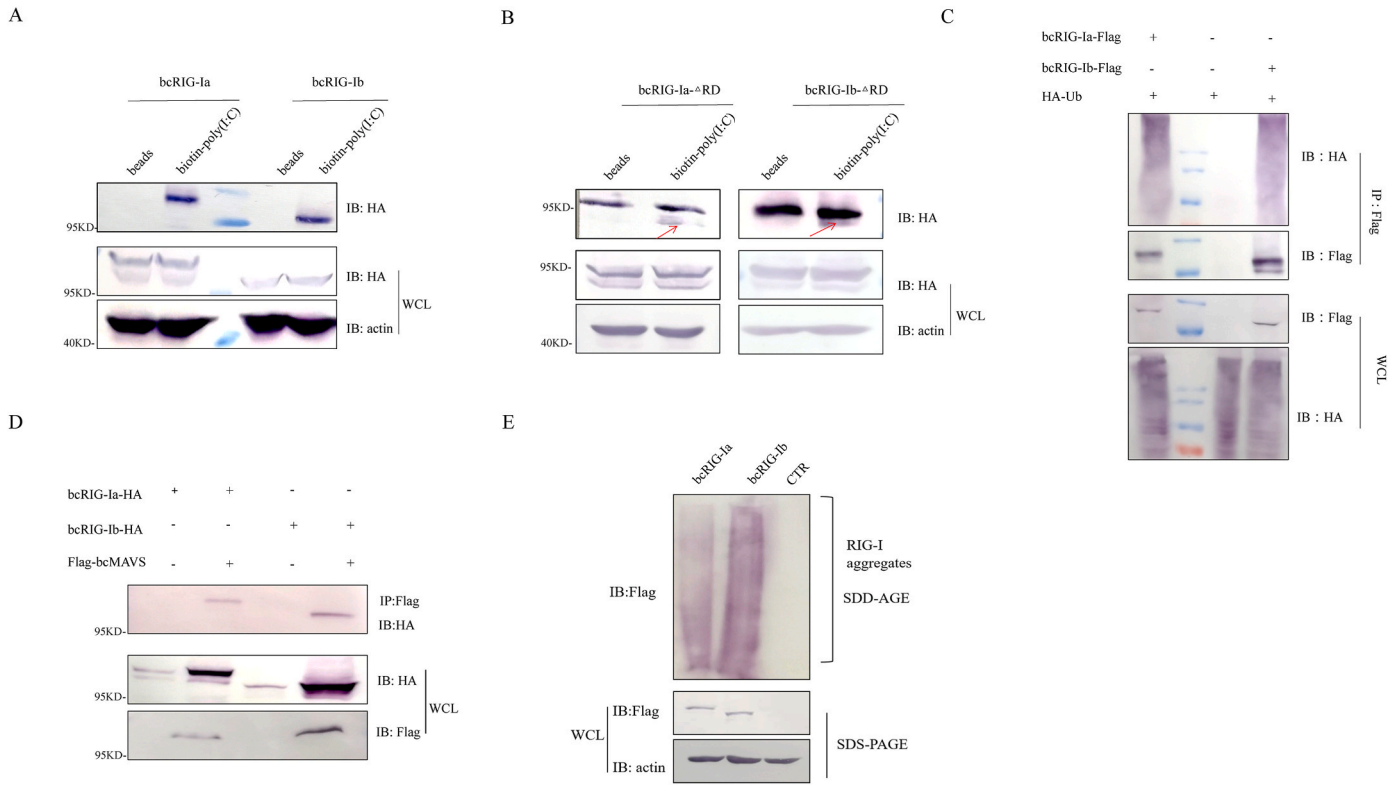

Fig. 3. RNA binding and oligomerization of bcRIG-Ia and bcRIG-Ib. HEK293T cells in 100 mm plate were transfected with bcRIG-Ia or bcRIG-Ib (A), or transfected with bcRIG-Ia-△RD (RD-deleted mutant) or bcRIG-Ib-△RD (15 μg), respectively (B). At 48 h after transfection, the cells were subjected to RNA pull-down assay. The lane labeled "Beads" corresponds to the experiment performed without biotinylated poly(I:C) (as control). (C) HEK293T cells in 100 mm plate were co-transfected with HA-Ub (7.5 μg) and bcRIG-Ia (bcRIG-Ib or empty vector) (7.5 μg), the transfected cells were harvested for co-IP at 48 h post transfection (hpt). (D) HEK293T cells in 100 mm plate were co-transfected with bcMAVS (10 μg) and bcRIG-Ia (bcRIG-Ib or empty vector) (5 μg), the transfected cells were harvested for co-IP at 48 hpt. (E) HEK293T cells in 100 mm plate were transfected with empty vector, bcRIG-Ia or bcRIG-Ib (15 μg) respectively, the transfected cells were harvested and analyzed by SDD-AGE (top) and SDS-PAGE (below) at 48 hpt separately. CTR: pcDNA5/FRT/TO; bcRIG-Ia-HA: pcDNA5/FRT/TO-bcRIG-Ia-HA; bcRIG-Ib-HA: pcDNA5/FRT/TO-bcRIG-Ib-HA; bcRIG-Ia-△RD-HA: pcDNA5/FRT/TO-bcRIG-Ia-△RD-HA; bcRIG-Ib-△RD-HA: pcDNA5/FRT/TO-bcRIG-Ib-△RD-HA; bcRIG-Ia-Flag: pcDNA5/FRT/TO-bcRIG-Ia-Flag; bcRIG-Ib-Flag: pcDNA5/FRT/TO-bcRIG-Ib-Flag; Flag-bcMAVS: pcDNA5/FRT/TO-Flag-bcMAVS; HA-Ub: pcDNA5/FRT/TO-HA-Ub.

bcRIG-Ia (GenBank accession number: OQ407684) and *bcRIG-Ib* (GenBank accession number: OQ407685), were cloned and identified from the spleen of black carp, which were composed of 2844 nucleotides and 2643 nucleotides, encoding 948 and 881 amino acids, respectively. To study the evolution of RIG-I, the amino acid sequence of bcRIG-Ia and bcRIG-Ib have been subjected to multiple alignments with those of RIG-I proteins from different species, including human (*Homo sapiens*), mouse (*Mus musculus*), duck (*Anas platyrhynchos*) and grass carp (*Ctenopharyngodon idella*) (Fig. 1A). Phylogenetic analysis was applied to bcRIG-I and RIG-I proteins of other known species, which was conducted by using MEGA 6.0 program (Fig. 1B). bcRIG-I shared high similarity with grass carp RIG-I (98.6%) and crucian carp (*Carassius auratus*) RIG-I (98.1%), and was clustered tightly with them, which correlated with the closest genetic relationship of these cyprinid fish (Fig. 1B and Table 2). Sequences analysis by using NCBI CDD (http://www. ncbi. nlm.nih.gov/Structure/cdd/docs/cdd_search.html) revealed that both bcRIG-Ia and bcRIG-Ib contained two N-terminal CARD domains, a central DExDc/H domain and a C-terminal RD domain (Fig. 1C). The RD domain of bcRIG-Ib was shorter (68 amino acids) than that of bcRIG-Ia, and there exist 4 different amino acids between bcRIG-Ia and bcRIG-Ib, 3 in the CARD domain (4, 5 and 28 sites) and 1in DExDc/H domain (464 site). Comparation among the RIG-I homologues from the selected species (Table 2) and the phylogenetic analysis (Fig. 1B) suggested the conservation of bcRIG-Ia/b in the vertebrates.

3.2. Protein expression and subcellular distribution of bcRIG-Ia and bcRIG-Ib

HEK293T cells and EPC cells were transfected with bcRIG-Ia or bcRIG-Ib independently, and the transfected cells were harvested and used for IB assay at 48 h post transfection separately. The specific band of around 104 KDa and 96 KDa, representing bcRIG-Ia or bcRIG-Ib respectively, were detected in the whole cell lysates from HEK293T cells and EPC cells expressing bcRIG-Ia-HA or bcRIG-Ib-HA, indicating that bcRIG-Ia and bcRIG-Ib were well expressed in both mammalian and fish cells (Fig. 2A). To examine the subcellular distribution of bcRIG-Ia and bcRIG-Ib, bcRIG-Ia-HA or bcRIG-Ib-HA was transfected into EPC cells, and used for immunofluorescent staining at 24 h after transfection, respectively. The fluorescent microscopy data revealed that bcRIG-Ia and bcRIG-Ib were distributed in both the cytolasm and the nucleus (Fig. 2B). At the same time, the transfected EPC cells used for nucleo-cytoplasmic separation. The subsequential IB assay showed that bcRIG-Ia and bcRIG-Ib were located in both cytoplasm and nucleus (Fig. 2C), which correlated with the result of immunofluorescence staining.

3.3. RNA binding and oligomerization of bcRIG-Ia and bcRIG-Ib

In mammals, the RD domain of RIG-I binds to viral RNA upon virus infection, which leads to the change of RIG-I conformation and promotes the formation of the RIG-I oligomers, which bind to MAVS to initiate

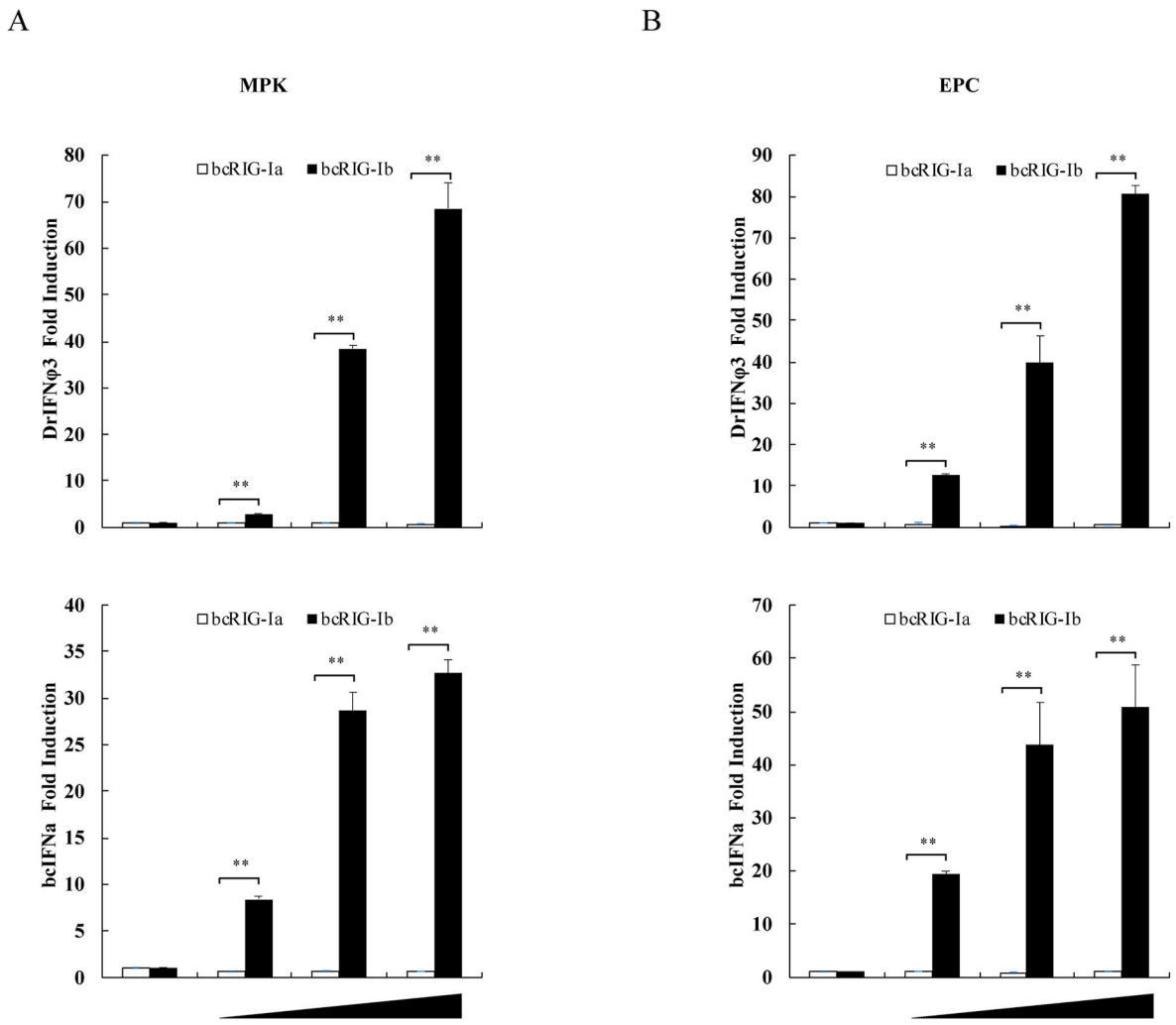

Fig. 4. The IFN-inducing activity of bcRIG-Ia and bcRIG-Ib. MPK cells (A) or EPC cells (B) in 24-well plate were co-transfected with pRL-TK (25 ng), Luci-DrIFNφ3 promoter or Luci-bcIFNa promoter (200 ng) and bcRIG-Ia or bcRIG-Ib(50 ng, 100 ng, 200 ng); The control group was transfected with empty vector (pcDNA5-FRT-TO); at 24 hpt, the cells were collected for dual-luciferase reporter gene assay. bcRIG-Ia: pcDNA5/FRT/TO-bcRIG-Ia-HA; bcRIG-Ib: pcDNA5/FRT/TO-bcRIG-Ib-HA.

downstream signaling pathways (Luo et al., 2011; Seth et al., 2005; Gack et al., 2007). The RNA pull-down assay revealed that both bcRIG-Ia and bcRIG-Ib could bind to synthetic poly(I:C) and showed the similar RNA-binding ability of bcRIG-Ia and bcRIG-Ib (Fig. 3A), which implied that both bcRIG-Ia and bcRIG-Ib were true cytoplasmic pattern recognition receptors. Meanwhile, bcRIG-Ia-△RD and bcRIG-Ib-△RD (truncation mutants lacking the RD domain) were able to bind to the synthetic poly(I:C); however, their RNA-binding ability was significantly weaker than wild type bcRIG-Ia and bcRIG-Ib (Fig. 3B , red arrow indicated). This result indicated that the C-terminal RD domain of bcRIG-Ia and bcRIG-Ib was crucial for recognition and binding of dsRNA. In addition, the ubiquitination and interaction with bcMAVS of bcRIG-Ia and bcRIG-Ib were tested. As shown in Fig. 3C, the co-immunoprecipitation (co-IP) assay and subsequential IB assay demonstrated that both bcRIG-Ia and bcRIG-Ib were modified with ubiquitination like their mammalian counterparty. And, both bcRIG-Ia and bcRIG-Ib were identified to be able to bind to bcMAVS (Fig. 3D). However, the SDD-AGE assay demonstrated that the oligomerization degree of bcRIG-Ia was obviously weaker than that of bcRIG-Ib (Fig. 3E).

3.4. The IFN signaling activated by bcRIG-Ia and bcRIG-Ib

To investigate the role of bcRIG-Ia and bcRIG-Ib in host IFN signaling pathway, MPK cells and EPC cells were transfected with bcRIG-Ia or bcRIG-Ib, and used for the reporter assay respectively. The transcription of DrIFNφ3 and bcIFNa promoter was activated by bcRIG-Ib but not bcRIG-Ia, which demonstrated that bcRIG-Ia and bcRIG-Ib played different roles in IFN signaling (Fig. 4A&B).

To further explore the role of bcRIG-Ia and bcRIG-Ib in host antiviral innate immune activation, MPK cells were transfected with bcRIG-Ia or bcRIG-Ib, and subjected to GCRV or SVCV infection (MOI = 0.01,0.1,1), respectively. The viral titers of the supernatant media were examined by the plaque assay, in which the viral titers of the cells transfected with bcRIG-Ia were similar to those of control, and the viral titers of the cells transfected with bcRIG-Ib were much lower to those of control (Fig. 5 A&B). At the same time, qRT-PCR assays were recruited to detect the mRNA levels of black carp *IFNb*, *Mx1*, *Viperin* and *SVCV* genes in the above cells. The mRNA levels of *bcIFNb*, *bcViperin*, *bcMx1* in the cells overexpressing bcRIG-Ib were much higher than those of the cells overexpressing bcRIG-Ia and the control, and accordingly, the mRNA levels of *SVCV-G*, *SVCV-N* and *SVCV-P* in the cells overexpressing bcRIG-Ib were much lower than those of the cells overexpressing bcRIG-Ia and the control (Fig. 5 C&D). Thus, overexpressed bcRIG-Ib, but not overexpressed bcRIG-Ia, could induce IFN production and offer the cells improved antiviral activity. Interestingly, bcRIG-Ia increased the mRNA levels of *SVCV-G*, *SVCV-N* and *SVCV-P*, compared to the control group

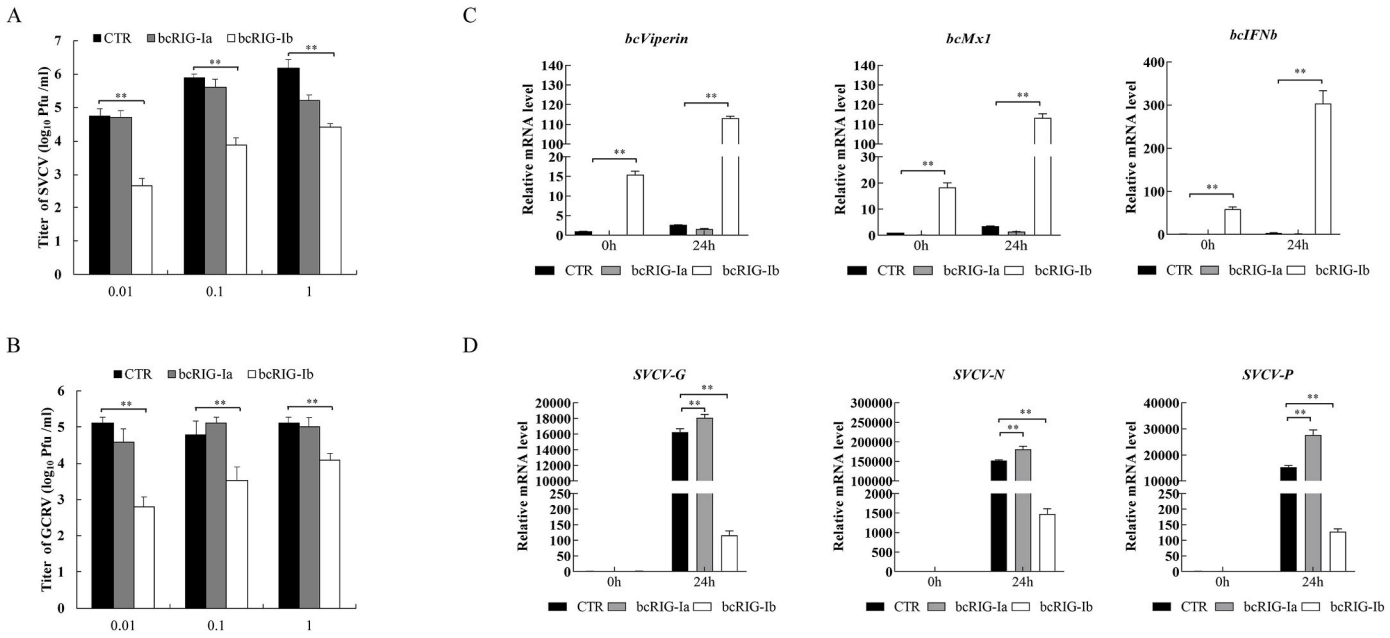

Fig. 5. The antiviral ability of bcRIG-Ia and bcRIG-Ib. MPK cells in 24-well plate were transfected with empty vector, bcRIG-Ia or bcRIG-Ib (300 ng) respectively, and the transfected cells were infected with SVCV(A) or GCRV(B) respectively. The supernatant was collected at 24 h post-infection (hpi) for virus titration. MPK cells in 6-well plate were transfected with empty vector, bcRIG-Ia or bcRIG-Ib (3 μg) respectively, and the transfected cells were infected with SVCV (MOI = 0.1). The relative mRNA levels of *bcIFNb*, bc*Mx1*, *bcViperin (C)* and *SVCV-G/P/N* (D)were examined by qRT-PCR at 24 hpi. CTR: pcDNA5/FRT/TO; bcRIG-Ia: pcDNA5/FRT/TO-bcRIG-Ia-HA; bcRIG-Ib: pcDNA5/FRT/TO-bcRIG-Ib-HA.

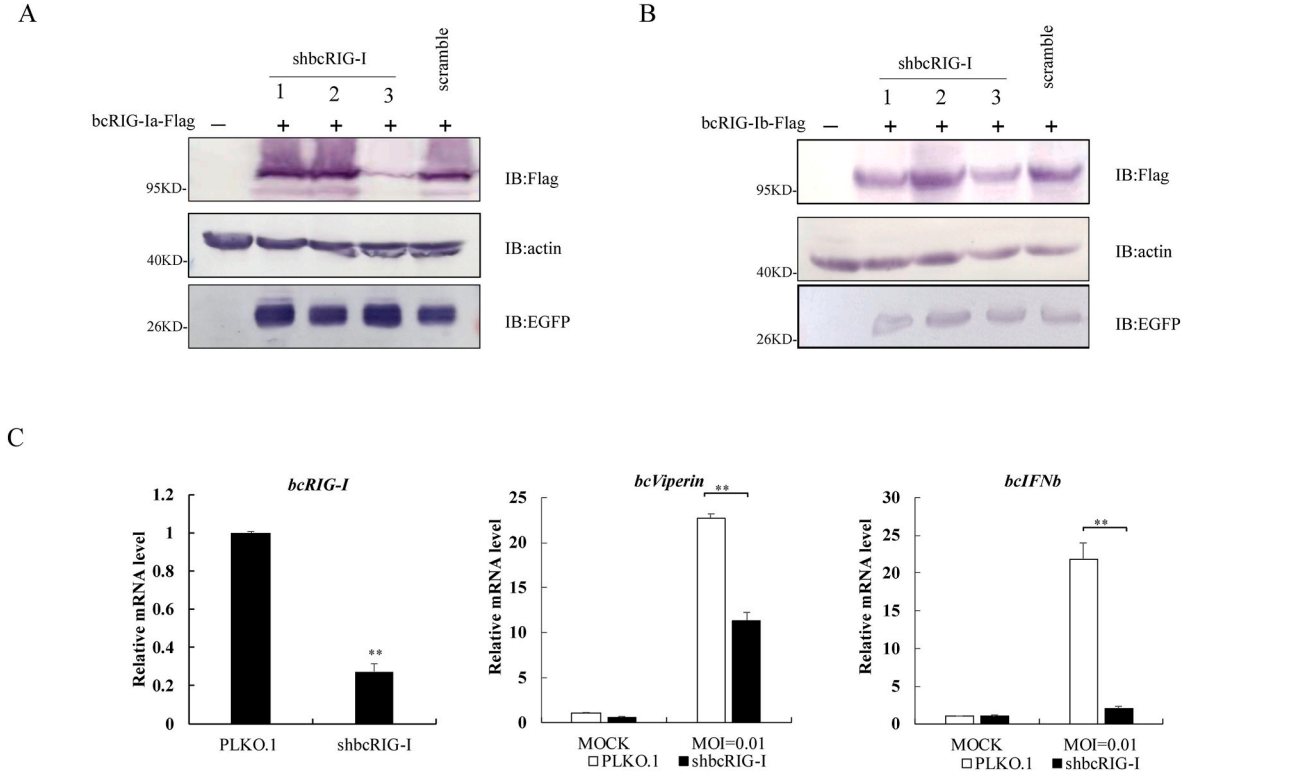

Fig. 6. bcRIG-I Knockdown inhibited SVCV triggered IFN and ISG production. (A&B) HEK293T cells in 6-well plate were co-transfected with bcRIG-Ia or bcRIG-Ib (1.5 μg) and shRNA targeting bcRIG-I (shbcRIG-I-1/2/3) (1.5 μg). The transfected cells were used for IB at 48 hpt. (C) MPK cells in 6-well plate were transfected with control shRNA (PLKO.1 scramble) or shbcRIG-I-3 (3 μg), respectively; which were infected with SVCV at 24 hpt. The transcription of *bcIFNb* or *bcViperin* was detected by qRT-PCR. bcRIG-Ia-Flag: pcDNA5/FRT/TO-bcRIG-Ia-Flag; bcRIG-Ib-Flag: pcDNA5/FRT/TO-bcRIG-Ib-Flag.

(Fig. 5D). We speculated that bcRIG-Ia might function as a negative regulator in the IFN signaling during the antiviral innate immune response.

To further confirm the role of bcRIG-Ia/b in host IFN production, shRNAs targeting both bcRIG-Ia and bcRIG-Ib were designed and their knockdown efficiency were tested by IB assay in HEK293T cells, in which shbcRIG-I-3 markedly reduced the expression of exogenous bcRIG-Ia and bcRIG-Ib (Fig. 6A&B). Subsequently, MPK cells transfected

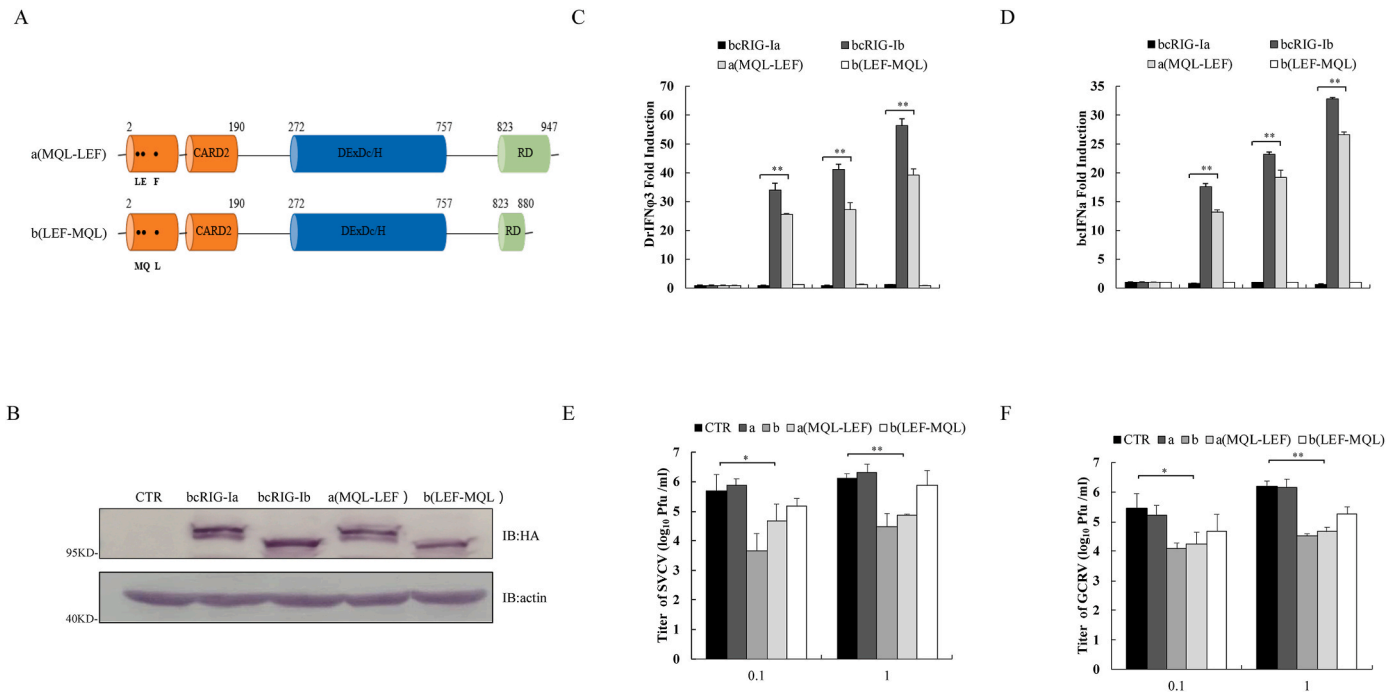

Fig. 7. CARD domain was crucial for bcRIG-I triggered IFN signaling. (A)The structural diagram of bcRIG-Ia (MQL-LEF) and bcRIG-Ib (LEF-MQL). (B) EPC cells in 6-well plate were transfected with bcRIG-Ia, bcRIG-Ib, bcRIG-Ia (MQL-LEF) bcRIG-Ib (LEF-MQL) or empty vector (3 μg), respectively. At 48 hpt, the protein expression was detected by IB. (C&D) MPK cells in 24-well plate were co-transfected with Luci-bcIFNa (200 ng) or Luci-DrIFNφ3 (200 ng), pRL-TK (25 ng), and bcRIG-Ia, bcRIG-Ib, bcRIG-Ia (MQL-LEF) or bcRIG-b (LEF-MQL) (50 ng, 100 ng, 200 ng), at 24 hpt, the cells were collected for dual-luciferase reporter gene assay. (E&F) MPK cells in 24-well plate were transfected with bcRIG-Ia, bcRIG-Ib, bcRIG-Ia (MQL-LEF) or bcRIG-Ib (LEF-MQL) (300 ng) respectively; at 24 hpt, the cells were infected with GCRV or SVCV (MOI = 0.1,1) separately. The cell supernatants were collected and detected by plaque assay at 24 hpi. a: pcDNA5/FRT/TO-bcRIG-Ia-HA; b: pcDNA5/FRT/TO-bcRIG-Ib-HA; a (MQL-LEF): pcDNA5/FRT/TO-bcRIG-Ia (MQL-LEF)-HA; b (LEF-MQL): pcDNA5/FRT/TO-bcRIG-I-b (LEF-MQL)-HA.

with shbcRIG-I-3 or control shRNA were subjected to SVCV infection (MOI = 0.01) and the mRNA levels of *bcIFNb* and *bcViperin* were determined by qRT-PCR. Over-expression of shbcRIG-I-3 led to 70% reduction of the bcRIG-I mRNA level and significant decrease of *bcIFNb* and *bcViperin* mRNA levels (Fig. 6C), which demonstrated that RIG-I knockdown dampened IFN signaling in black carp.

3.5. CARD domain was crucial for bcRIG-I triggered IFN signaling

To decipher the mechanism behind the difference between bcRIG-Ia and bcRIG-Ib in IFN signaling. Multi-site mutants of RIG-I, bcRIG-Ia (MQL-LEF) and bcRIG-Ib (LEF-MQL), were constructed and their expression were identified by IB assay, since the 2CARD domains are crucial for the activation of RIG-I in mammals (Fig. 7A&B). Next, the luciferase reporter assay in MPK cells showed that bcRIG-Ia (MQL-LEF) mutant presented similar ability to induce the transcription of both bcIFNa promoter and DrIFNφ3 promoter to that of bcRIG-Ib, whereas bcRIG-Ib (LEF-MQL) almost lost the ability to activate the transcription of the IFN promoters, just like bcRIG-Ia (Fig. 7C&D). At the same time, the antiviral activity of bcRIG-Ia/b and above mutants were measured and compared by plaque assay. Both GCRV and SVCV titers in the supernatant media of the cells transfected with bcRIG-Ib or bcRIG-Ia (MQL-LEF) were markedly lower than those of the cells transfected with bcRIG-Ia or bcRIG-Ib (LEF-MQL) (Fig. 7E&F), which correlated with the reporter assay data. These results further suggested that amino acids at sites 4,5 and 28 in the CARD domain, but not the 464 site in the DExDc/H domain, were crucial for bcRIG-Ib-mediated antiviral signaling.

3.6. Phenylalanine-28 was essential for bcRIG-Ib mediated IFN signaling

According to the above results, the functional difference between bcRIG-Ia and bcRIG-Ib in IFN signaling was due to the different amino acid 4,5 and 28 in the CARD domain. So, the single-site mutants, including bcRIG-Ia (M4L), bcRIG-Ia (Q5E) and bcRIG-Ia (L28F), were constructed and characterized by IB assay in EPC cells (Fig. 8A&B). Then, MPK cells were transfected with bcRIG-Ia or bcRIG-Ia single-site mutants separately, and used for reporter assay. The result showed that bcRIG-Ia (L28F), but not bcRIG-Ia (M4L) or bcRIG-Ia (Q5E), potently induced the transcription of bcIFNa promoter (Fig. 8C), implying the essential of F28. Based on this, the single-site mutant, bcRIG-Ib (F28L), was constructed and characterized by IB assay in EPC cells (Fig. 8B). And the reporter assay demonstrated that, compared with wild type bcRIG-Ib, bcRIG-Ib (F28L) almost lost the IFN-inducing ability (Fig. 8C). The subsequential plaque assay identified that bcRIG-Ia (L28F) presented similar antiviral activity to that of bcRIG-Ib. And, bcRIG-Ib (F28L), like wild type bcRIG-Ia, almost had no antiviral activity (Fig. 8E).

To further confirm the "role" of F28, the plasmids expressing the 2CARD domain of wild type bcRIG-Ia/b or above single-site mutants were constructed and used for the reporter assay and plaque assay separately. Consistently, over-expression of bcRIG-Ia-CARD (L28F) markedly increased the activity of bcIFNa promoter as well as bcRIG-Ib-CARD; however, bcRIG-Ia-CARD, bcRIG-Ia-CARD (M4L) and bcRIG-Ia-CARD (Q5E) showed little IFN-inducing ability (Fig. 8D). In line with this result, the plaque assay identified that bcRIG-Ia-CARD (L28F) obtained similar antiviral activity to that of bcRIG-Ib-CARD, and bcRIG-Ia-CARD, bcRIG-Ia-CARD (M4L) and bcRIG-Ia-CARD (Q5E) showed little antiviral activity (Fig. 8F). These results collectively indicated that F28 was essential for bcRIG-Ib mediated antiviral signaling.

3.7. Phenylalanine-28 was important for the oligomerization of black carp RIG-I

The CARD domain is crucial for RIG-I to activate downstream signaling in mammals. And our data demonstrated that F28 in CARD domain of black carp RIG-I was essential for it triggered IFN signaling.

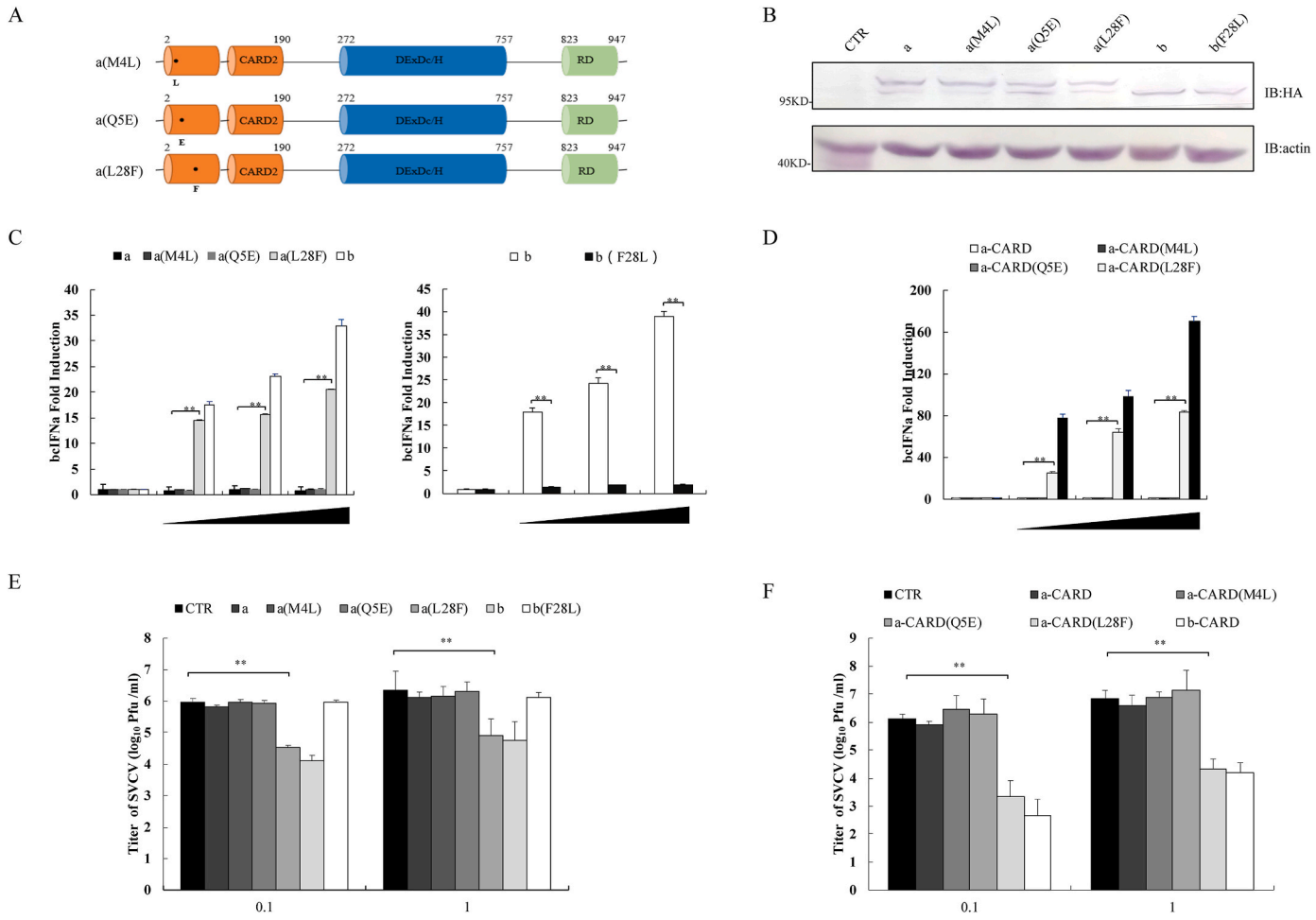

Fig. 8. F28 was crucial for bcRIG-Ib mediated antiviral signaling. Diagrams (A) and IB (B) of the single-site mutants of bcRIG-Ia/b. (C) MPK cells in 24-well plate co-transfected with pRL-TK (25 ng), Luci-bcIFNa (200 ng), bcRIG-Ia, bcRIG-Ib, or indicated mutants (50 ng, 100 ng, 200 ng) and used for dual-luciferase reporter gene assay at 24 hpt, respectively. (D) MPK cells in 24-well plate were co-transfected with pRL-TK (25 ng), Luci-bcIFNa (200 ng), bcRIG-Ia-CARD, bcRIG-Ib-CARD, or indicated mutants (50 ng, 100 ng, 200 ng), and used for dual-luciferase reporter gene assay at 24 hpt, respectively. MPK cells in 24-well plate were transfected with bcRIG-Ia, bcRIG-Ib or indicated mutants (300 ng) (E), or transfected with bcRIG-Ia-CARD, bcRIG-Ib-CARD or indicated mutants (300 ng) (F). At 24 h after SVCV (MOI = 0.1, 1) infection, the cell supernatants were collected and the virus titer was detected by plaque assay. a: pcDNA5/FRT/TO-bcRIG-Ia-HA; b: pcDNA5/FRT/TO-bcRIG-Ib-HA; a (M4L): pcDNA5/FRT/TO-bcRIG-Ia (M4L)-HA; a (Q5E): pcDNA5/FRT/TO-bcRIG-Ia (Q5E)-HA; a (L28F): pcDNA5/FRT/TO-bcRIG-Ia (L28F)-HA; b (F28L): pcDNA5/FRT/TO-bcRIG-Ib(F28L)-HA; a-CARD: pcDNA5/FRT/TO-bcRIG-Ia-CARD-HA; b-CARD: pcDNA5/FRT/TO-bcRIG-Ib-CARD-HA; a-CARD (M4L): pcDNA5/FRT/TO-bcRIG-Ia-CARD (M4L)-HA; a-CARD (Q5E): pcDNA5/FRT/TO-bcRIG-Ia-CARD (Q5E)-HA; a-CARD (L28F): pcDNA5/FRT/TO-bcRIG-Ia-CARD (L28F)-HA.

To explore whether the functional difference between bcRIG-Ia and bcRIG-Ib in IFN production is due to the structural change of the CARD domain, structural analysis by using https://robetta.bakerlab.org/was recruited to compare the structures of CARD domains of bcRIG-Ia, bcRIG-Ib and their mutants. The data showed that there was no obvious structural change between bcRIG-Ia-CARD and bcRIG-Ia-CARD (L28F) (Fig. 9A), or between bcRIG-Ib-CARD and bcRIG-Ib-CARD (F28L) (Fig. 9B), indicating the difference at site 28 between bcRIG-Ia-CARD and bcRIG-Ib-CARD did not affect their structure (Fig. 9A&B). The formation of oligomer is a critical step for RIG-I activation, which triggers us to test whether the different aa of 28 site leads to the different oligomerization of bcRIG-Ia and bcRIG-Ib. The result of SDD-AGE showed that the oligomerization degree of bcRIG-Ib was obviously stronger than bcRIG-Ia, and bcRIG-Ia (L28F) oligomer was much heavier than that of bcRIG-Ib (F28L) (Fig. 9C). Thus, our data demonstrated that F28 was crucial for the oligomerization and subsequential activation of bcRIG-Ib.

3.8. Phenylalanine-28 was crucial for RIG-I mediated IFN signaling in cyprinid fish

To further determine whether the mechanism of F28 of bcRIG-Ib was conserved in teleost fishes, the amino acid sequences of CARD of RIG-Is from different teleost species were compared, including black carp, grass carp (*C. idella*), common carp (*C. carpio*), crucian carp (*C.auratus*), zebrafish (*D. rerio*), Atlantic salmon (*S. salar*) and rainbow trout (*O. mykiss*), which suggested that phenylalanine-28 was conserved among teleost fishes (Fig. 10A). Next, plasmids expressing RIG-I from grass carp (CiRIG-I), EPC cells (eRIG-I), zebrafish (DrRIG-I), or their single-site mutants, including CiRIG-I (F28L), eRIG-I (F28L), DrRIG-Ib (F28L) were constructed separately. The reporter assay showed that all the F28L mutants of the above RIG-Is lost the ability to induce the transcription of IFN promoter, compared with the wild type RIG-Is (Fig. 10B&C). Based on this, plasmids expressing CARD domain of

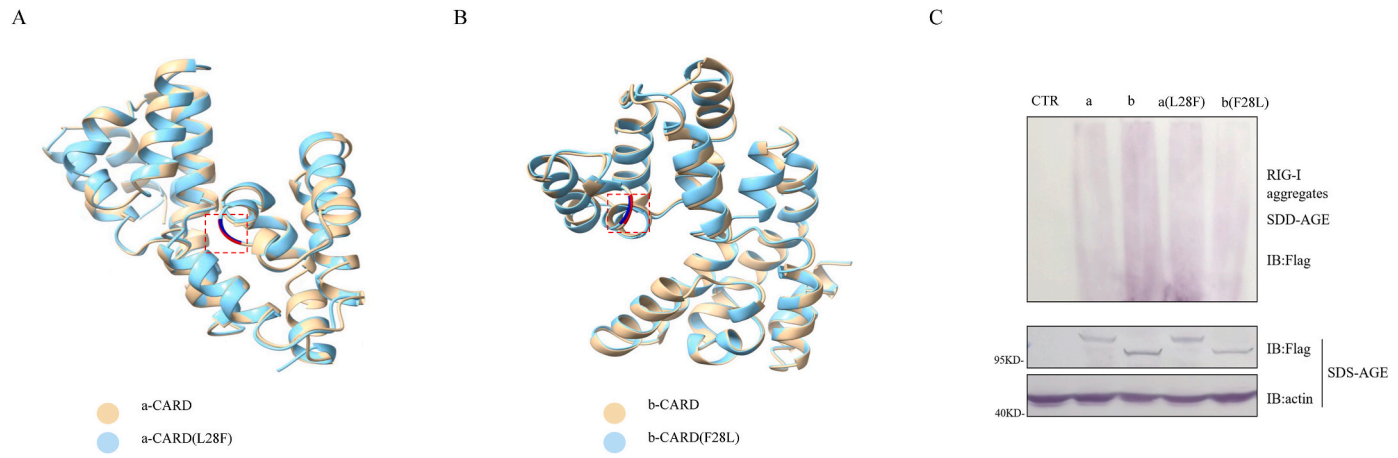

Fig. 9. F28 was crucial for the oligomerization of bcRIG-I. (A&B) The predicted structures of bcRIG-Ia-CARD, bcRIG-Ia-CARD (L28F), bcRIG-Ib-CARD or bcRIG-Ib-CARD (F28L) (by https://robetta.bakerlab.org/). (C) HEK293T cells in 100 mm were transfected with bcRIG-Ia, bcRIG-Ib, bcRIG-Ia (L28F) or bcRIG-Ib(F28L) (15 μg), respectively. At 48 hpt, the oligomerization of bcRIG-Ia, bcRIG-Ib, bcRIG-Ia (L28F) or bcRIG-Ib (F28L) was examined by SDD-AGE. a: pcDNA5/FRT/TO-bcRIG-Ia-Flag; b: pcDNA5/FRT/TO-bcRIG-Ib-Flag; a (L28F): pcDNA5/FRT/TO-bcRIG-Ia (L28F)-Flag; b (F28L): pcDNA5/FRT/TO-bcRIG-Ib (F28L)-Flag.

above RIG-Is and above RIG-I mutants were constructed separately, and subsequential reporter assay identified that CiRIG-I-CARD, eRIG-I-CARD and DrRIG-I-CARD showed strong ability to induce the transcription of bcIFNa promoter and eIFN promoter. And consistently, the IFN-inducing ability of CiRIG-I-CARD (F28L), eRIG-I-CARD (F28L) and DrRIG-I-CARD (F28L) was markedly dampened (Fig. 10D&E). These results collectively suggested that phenylalanine-28 was essential for RIG-I mediated IFN signaling in cyprinid fish.

4. Discussion

RIG-I was first identified during the differentiation of NB4 cells in 1997 (Sun, 1997), and was identified as a cytoplasmic viral RNA sensor that triggered the production of type I IFNs and pro-inflammatory cytokines during viral infection in 2004 (Yoneyama et al., 2004). So far, the function of RIG-I and its regulatory mechanism in innate immunity have been extensively investigated. RLRs in teleost fish, when being transcribed, may be spliced at RNA levels, leading to the sequence deletion or insertion in some functional domains. In previous study, two spliced transcripts of RIG-I have been identified in both zebrafish (Zou et al., 2015) and Japanese eel (Huang et al., 2019). In this study, a typical type as well as a deletion variant of RIG-I with 68 amino acids deleted in the C-terminal RD domain, named bcRIG-Ia and bcRIG-Ib respectively, were also identified and characterized in black carp. Besides, there are four different amino acids, site 4, 5, 28 in CARD domain and site 464 in DExDc/H domain, between bcRIG-Ia and bcRIG-Ib (Fig. 1).

In mammals, all RLR members have been proved to possess RNA-binding activity (Wilkins and Gale, 2010). In teleost, rainbow trout MDA5 and LGP2 have been identified to bind synthetic dsRNA poly (I:C) (Chang et al., 2011). However, there still no report about the RNA-binding activity of teleost RIG-I. In our study, RNA pull-down assay proved that both bcRIG-Ia and bcRIG-Ib could bind to synthetic poly(I:C), implying that black carp RIG-I was a cytosolic pattern recognition receptor in a true sense. RIG-I has long been known to be a receptor that recognizes viral RNA in the cytoplasm. However, researchers discovered the existence of RIG-I in the nucleus in 2018, which can recognize the replicating IAV in the nucleus and induce the production of type I IFNs, thus establishing an effective antiviral state to limit the replication of IAV (Liu et al., 2018). In this study, the results of immunofluorescence and nuclear and cytoplasmic protein extraction showed that bcRIG-Ia and bcRIG-Ib were distributed in both cytoplasm and nucleus, which correlated with the data of mammalian RIG-I. However, the roles of bcRIG-Ia and bcRIG-Ib in the nucleus still need to be further explored.

In mammals, upon recognition of viral RNA, E3-ubiquitin ligase TRIM25 delivers a k63-linked polyubiquitin chain to the second CARD domain of RIG-I and the ubiquitination facilitates the oligomerization of RIG-I and subsequent interaction with MAVS to initiate the antiviral signaling cascade (Zen et al., 2010; Gack et al., 2008; Ohman et al., 2009). In the present study, both bcRIG-Ia and bcRIG-Ib could undergo ubiquitination modification. Moreover, co-IP assay showed that both bcRIG-Ia and bcRIG-Ib could interact with bcMAVS, and the C-terminal RD domain of bcRIG-Ia and bcRIG-Ib was crucial for recognition and binding of dsRNA(Fig. 3). These results suggested that the activation mechanism of RIG-I in IFN signaling pathway in black carp was similar to that of its mammalian counterpart. In mammals, only activated RIG-I translocated to mitochondria and interacted with MAVS, leading to the activation of MAVS/IFN cascade. However, the data in this study demonstrated that, bcRIG-Ia, although showing no ability to trigger the IFN signaling, could bind to bcMAVS in the co-IP assay (Fig. 3D), which implying the difference in RLR/IFN regulation between lower vertebrates and higher vertebrates.

Actually, bcRIG-Ib, but not bcRIG-Ia, induced transcription of type I IFNs and ISGs, thus protecting host cells against SVCV and GCRV infection. The mutation experiments identified that F28 of bcRIG-Ib was crucial for the oligmerization of bcRIG-Ib(Fig. 9C), which explained the functional difference between bcRIG-Ia and bcRIG-Ib. It was interesting that F28 was conserved among teleost fish, and the site mutation assay determined that F28 was crucial for cyprinid RIG-I mediated IFN signaling(Fig. 10), which further suggested the conservation of innate immune regulation in lower vertebrates, such as teleost fish.

Data availability

Data will be made available on request.

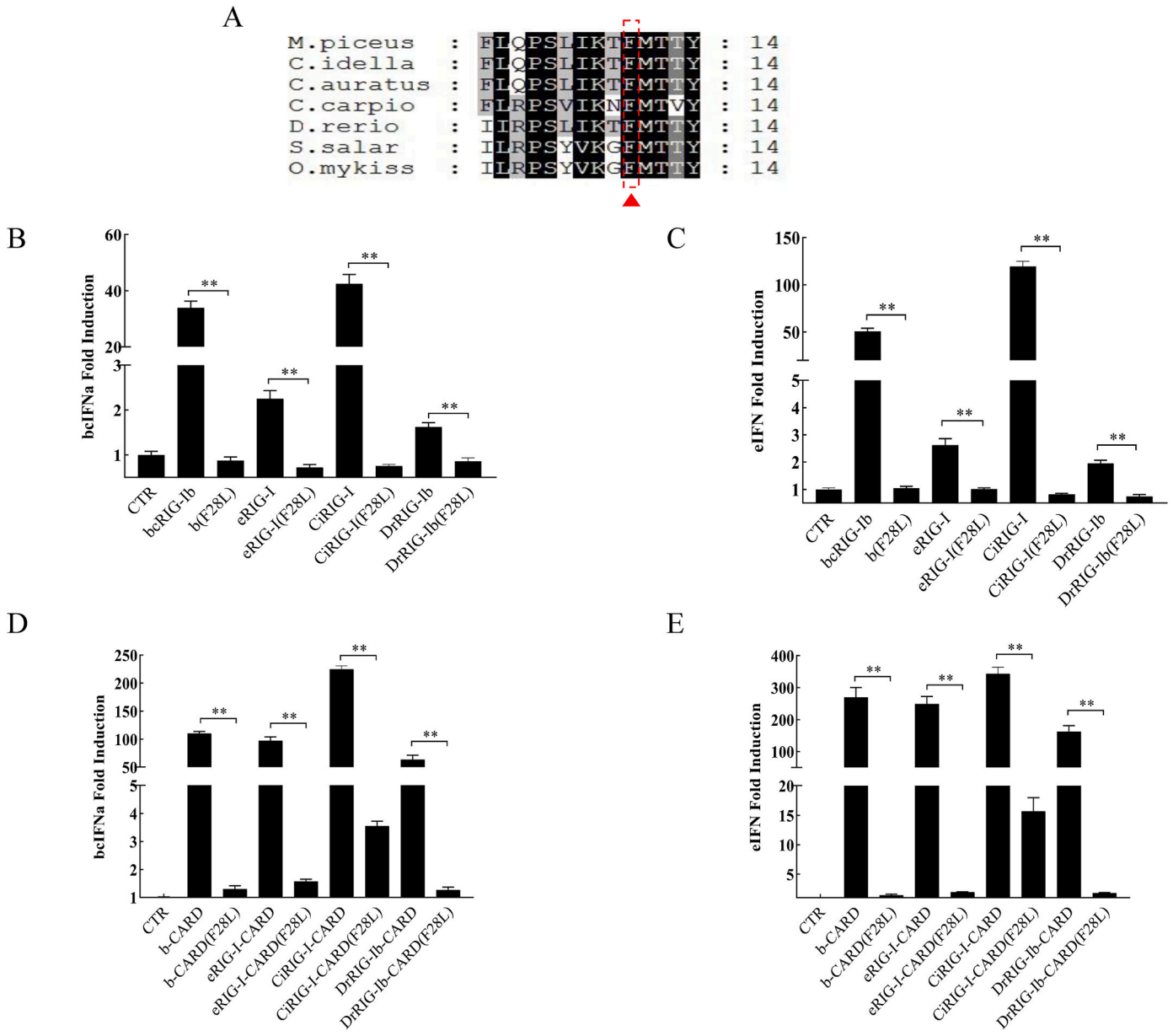

Fig. 10. Role of F28 of RIG-I in cyprinid fish. (A) Sequence alignment of CARD domain of RIG-I revealed conserved phenylalanine site F28 in *C. idella* (JX649222.1), *M. piceus b* (OQ407685), *C. auratus* (JF970225.1), *C. carpio* (HQ850439.1), *S.salar* (NM_001163699.1) and *O.mykiss* (FN178459.2) by using MEGA 6.0 program and GeneDoc program. pRL-TK (25 ng) and Luci-bcIFNa promoter (200 ng)or Luci-eIFN promoter (200 ng) were co-transfected into EPC cells in 24-well plate with wild type RIG-Is or RIG-I (F28L) mutants (200 ng) (B&C), and CARD domain or RIG-I-CARD (F28L) mutants (200 ng) (D&E) in cyprinid fish. After 24 h transfection, the cells were used for dual-luciferase reporter assay. bcRIG-Ib : pcDNA5/FRT/TO-bcRIG-Ib-Flag; b (F28L): pcDNA5/FRT/TO-bcRIG-Ib (F28L)-Flag; eRIG-I: pcDNA5/FRT/TO-Flag-eRIG-I; eRIG-I (F28L): pcDNA5/FRT/TO-Flag-eRIG-I (F28L); CiRIG-I: pcDNA5/FRT/TO-CiRIG-I-Flag; CiRIG-I(F28L): pcDNA5/FRT/TO-CiRIG-I (F28L)-Flag; DrRIG-Ib: pcDNA5/FRT/TO-Flag-DrRIG-Ib; DrRIG-Ib (F28L): pcDNA5/FRT/TO-Flag-DrRIG-Ib (F28L); b-CARD:pcDNA5/FRT/TO-bcRIG-Ib-CARD-Flag b-CARD (F28L): pcDNA5/FRT/TO-bcRIG-Ib-CARD (F28L)-Flag; eRIG-I-CARD: pcDNA5/FRT/TO-Flag-eRIG-I-CARD; eRIG-I-CARD (F28L): pcDNA5/FRT/TO-Flag-eRIG-I-CARD (F28L); CiRIG-I-CARD: pcDNA5/FRT/TO-CiRIG-I-CARD-Flag; CiRIG-I-CARD (F28L): pcDNA5/FRT/TO-CiRIG-I-CARD (F28L)-Flag; DrRIG-Ib-CARD: pcDNA5/FRT/TO-Flag-DrRIG-Ib-CARD; DrRIG-Ib-CARD (F28L): pcDNA5/FRT/TO-Flag-DrRIG-Ib-CARD (F28L).

Acknowledgements

This work was supported by the National Natural Science Foundation of China (U21A20268, 31920103016), Hunan Provincial Science and Technology Department (2021NK2025, 2022JJ40271), the Modern Agricultural Industry Program of Hunan Province, China Postdoctoral Science Foundation (2022M721126), and the Fish Disease, Vaccine Research and Development Platform for Postgraduates in Hunan Province.

Appendix A. Supplementary data

Supplementary data to this article can be found online at https://doi.org/10.1016/j.dci.2023.104917.

References

Akira, S., Uematsu, S., Takeuchi, O., 2006. Pathogen recognition and innate immunity. Cell 124 (4), 783–801.

Broz, P., Monack, D.M., 2013. Newly described pattern recognition receptors team up against intracellular pathogens. Nat. Rev. Immunol. 13 (8), 551–565.

Chang, M.X., Collet, B., Nie, P., Lester, K., Campbell, S., Secombes, C.J., Zou, J., 2011. Expression and functional characterization of the RIG-I-like receptors MDA5 and LGP2 in Rainbow trout (Oncorhynchus mykiss). J. Virol. 85 (16), 8403–8412.
Chen, H.Y., Liu, W.T., Wu, S.Y., Chiou, P.P., Li, Y.H., Chen, Y.C., Lin, G.H., Lu, M.W., Wu, J.L., 2015. RIG-I specifically mediates group II type I IFN activation in nervous necrosis virus infected zebrafish cells. Fish Shellfish Immunol. 43 (2), 427–435.
Chen, L., Su, J.G., Yang, C.R., Peng, L.M., Wan, Q.Y., Wang, L., 2012. Functional characterizations of RIG-I to GCRV and viral/bacterial PAMPs in grass carp Ctenopharyngodon idella. PLoS One 7 (7), e42182.
Elward, K., Gasque, P., 2003. "Eat me" and "don't eat me" signals govern the innate immune response and tissue repair in the CNS: emphasis on the critical role of the complement system. Mol. Immunol. 40 (2–4), 85–94.
Gack, M.U., Kirchhofer, A., Shin, Y.C., Inn, K.S., Liang, C., Cui, S., Myong, S., Ha, T., Hopfner, K.P., Jung, J.U., 2008. Roles of RIG-I N-terminal tandem CARD and splice variant in TRIM25-mediated antiviral signal transduction. Proc. Natl. Acad. Sci. U.S. A. 105 (43), 16743–16748.
Gack, M.U., Shin, Y.C., Joo, C.H., Urano, T., Liang, C., Sun, L., Takeuchi, O., Akira, S., Chen, Z., Inoue, S., Jung, J.U., 2007. TRIM25 RING-finger E3 ubiquitin ligase is essential for RIG-I-mediated antiviral activity. Nature 446 (7138), 916–920.
Hou, F.J., Sun, L.J., Zheng, H., Skaug, B., Jiang, Q.X., Chen, Z.J., 2011. MAVS forms functional prion-like aggregates to activate and propagate antiviral innate immune response. Cell 146 (3), 448–461.
Huang, B., Wang, Z.X., Zhang, C., Zhai, S.W., Han, Y.S., Huang, W.S., Nie, P., 2019. Identification of a novel RIG-I isoform and its truncating variant in Japanese eel, Anguilla japonica. Fish Shellfish Immunol. 94, 373–380.
Kato, H., Takeuchi, O., Sato, S., Yoneyama, M., Yamamoto, M., Matsui, K., Uematsu, S., Jung, A., Kawai, T., Ishii, K.J., Yamaguchi, O., Otsu, K., Tsujimura, T., Koh, C.S., Reis, e.Sousa, Matsuura, Y., Fujita, T., Akira, S., 2006. Differential roles of MDA5 and RIG-I helicases in the recognition of RNA viruses. Nature 441 (7089), 101–105.
Kolakofsky, D., Kowalinski, E., Cusack, S., 2012. A structure-based model of RIG-I activation. RNA 18 (12), 2118–2127.
Kowalinski, E., Lunardi, T., McCarthy, A.A., Louber, J., Brunel, J., Grigorov, B., Gerlier, D., Cusack, S., 2011. Structural basis for the activation of innate immune pattern-recognition receptor RIG-I by viral RNA. Cell 147 (2), 423–435.
Leung, D.W., Amarasinghe, G.K., 2012. Structural insights into RNA recognition and activation of RIG-I-like receptors. Curr. Opin. Struct. Biol. 22 (3), 297–303.
Liu, G., Lu, Y., Thulasi, Raman S.N., Xu, F., Wu, Q., Li, Z., Brownlie, R., Liu, Q., Zhou, Y., 2018. Nuclear-resident RIG-I senses viral replication inducing antiviral immunity. Nat. Commun. 9 (1), 3199.
Liu, J., Cao, X.T., 2016. Cellular and molecular regulation of innate inflammatory responses. Cell. Mol. Immunol. 13 (6), 711–721.
Luo, D., Ding, S.C., Vela, A., Kohlway, A., Lindenbach, B.D., Pyle, A.M., 2011. Structural insights into RNA recognition by RIG-I. Cell 147 (2), 409–422.
Meylan, E., Tschopp, J., Karin, M., 2006. Intracellular pattern recognition receptors in the host response. Nature 442 (7098), 39–44.
Ohman, T., Rintahaka, J., Kalkkinen, N., Matikainen, S., Nyman, T.A., 2009. Actin and RIG-I/MAVS signaling components translocate to mitochondria upon influenza A virus infection of human primary macrophages. J. Immunol. 182 (9), 5682–5692.
Peisley, A., Wu, B., Yao, H., Walz, T., Hur, S., 2013. RIG-I forms signaling-competent filaments in an ATP-dependent, ubiquitin-independent manner. Mol. Cell. 51 (5), 573–583.
Saito, T., Hirai, R., Loo, Y.M., Owen, D., Johnson, C.L., Sinha, S.C., Akira, S., Fujita, T., Gale Jr., M., 2007. Regulation of innate antiviral defenses through a shared repressor domain in RIG-I and LGP2. Proc. Natl. Acad. Sci. U.S.A. 104 (2), 582–587.
Stetson, D.B., Medzhitov, R., 2006. Type I interferons in host defense. Immunity 25 (3), 373–381.
Seth, R.B., Sun, L., Ea, C.K., Chen, Z.J., 2005. Identification and characterization of MAVS, a mitochondrial antiviral signaling protein that activates NF-kappaB and IRF3. Cell 122 (5), 669–682.
Sun, Y., 1997. RIG-I, a Homolog Gene of RNA Helicase, Is Induced by Retinoic Acid during the Differentiation of Acute Promyelocytic Leukemia Cell (PhD Thesis). Shanhai Institute of Heamatology, Rui-Jin Hospital, Shanghai Second Medical University[J].
Takeuchi, O., Akira, S., 2010. Pattern recognition receptors and inflammation. Cell 140 (6), 805–820.
Vegna, S., Gregoire, D., Moreau, M., Lassus, P., Durantel, D., Assenat, E., Hibner, U., Simonin, Y., 2016. NOD1 participates in the innate immune response triggered by hepatitis C virus polymerase. J. Virol. 90 (13), 6022–6035.
Wang, C.Y., Li, J., Yang, X., Wang, Q., Zhong, H.J., Liu, Y.K., Yan, W., He, Y.F., Deng, Z. Y., Xiao, J., Feng, H., 2021. Black carp IKKε collaborates with IRF3 in the antiviral signaling. Fish Shellfish Immunol. 118, 160–168.
Wilkins, C., Gale Jr., M., 2010. Recognition of viruses by cytoplasmic sensors. Curr. Opin. Immunol. 22 (1), 41–47.
Wu, H., Zhang, Y.Y., Lu, X.Y., Xiao, J., Feng, P.H., Feng, H., 2019. STAT1a and STAT1b of black carp play important roles in the innate immune defense against GCRV. Fish Shellfish Immunol. 87, 386–394.
Yang, C., Liu, L.Q., Liu, J., Ye, Z., Wu, H., Feng, P.H., Feng, H., 2019. Black carp IRF5 interacts with TBK1 to trigger cell death following viral infection. Dev. Comp. Immunol. 100, 103426.
Yoneyama, M., Kikuchi, M., Matsumoto, K., Imaizumi, T., Miyagishi, M., Taira, K., Foy, E., Loo, Y.M., Gale Jr., M., Akira, S., Yonehara, S., Kato, A., Fujita, T., 2005. Shared and unique functions of the DExD/H-box helicases RIG-I, MDA5, and LGP2 in antiviral innate immunity. J. Immunol. 175 (5), 2851–2858.
Yoneyama, M., Kikuchi, M., Natsukawa, T., Shinobu, N., Imaizumi, T., Miyagishi, M., Taira, K., Akira, S., Fujita, T., 2004. The RNA helicase RIG-I has an essential function in double-stranded RNA-induced innate antiviral responses. Nat. Immunol. 5 (7), 730–737.
Zen, W., Sun, L., Jiang, X., Chen, X., Hou, F., Adhikari, A., Xu, M., Chen, Z.J., 2010. Reconstitution of the RIG-I pathway reveals a signaling role of unanchored polyubiquitin chains in innate immunity. Cell 141 (2), 315–330.
Zhou, W., Zhou, J., Lv, Y., Qu, Y.X., Chi, M.D., Li, J., Feng, H., 2015. Identification and characterization of MAVS from black carp Mylopharyngodon piceus. Fish Shellfish Immunol. 43 (2), 460–468.
Zou, P.F., Chang, M.X., Li, Y., Zhang, S.H., Fu, J.P., Chen, S.N., Nie, P., 2015. Higher antiviral response of RIG-I through enhancing RIG-I/MAVS-mediated signaling by its long insertion variant in zebrafish. Fish Shellfish Immunol. 43 (1), 13–24.